

Upconversion emission of BaTiO₃:Er nanocrystals

PUSHPAL GHOSH, SUPARNA SADHU, TAPASI SEN and AMITAVA PATRA*

Department of Materials Science and Centre for Advanced Materials, Indian Association for the Cultivation of Science, Kolkata 700 032, India

Abstract. Here, we report the dopant concentration and pump-power dependence upconversion emission properties of erbium doped BaTiO₃ nanocrystals derived from sol-emulsion-gel method. Green (550 nm) and red (670 nm) upconversion emissions were observed at room temperature from the ⁴S_{3/2} and ⁴F_{9/2} levels of Er³⁺:BaTiO₃ nanocrystals. It is found that at 850 mW of cw excitation power (at 980 nm) the total luminescence was 17130 Cd/m² for 1000°C heated 0.25 mol% Er-doped BaTiO₃ nanocrystals. It is worthwhile to mention that the unusual power-dependent upconversion luminescence (saturation) is observed at higher dopant concentration (2.5 mol%) and high pump power. Our analysis confirms that the depletion of the excited state is responsible for the relevant fluorescence upconversion. We have again confirmed that a two-photon excited state absorption process occurs for all samples.

Keywords. Nanocrystals; erbium; upconversion; two-photon excitation.

1. Introduction

The research in the field of rare-earth doped nanocrystals for upconversion emission has recently been paid great attention to find out potential applications in the areas of photonic and biophotonic (Silversmith *et al* 1987; Downing *et al* 1996). As these potential applications are still very much in the design-phase, further fundamental research in the field of upconversion spectroscopy remains a challenge. Intensive research efforts are, therefore, devoted to designing and tuning of the upconversion properties of these materials. As a matter of fact, upconversion emissions of rare-earth ions-doped nanocrystals have already been shown in different crystal hosts such as ZrO₂ (Patra *et al* 2003a), Y₂O₃ (Matsuura 2002; La-Rosa-Cruz *et al* 2003), Lu₂O₃ (Pandozzi *et al* 2005; La Rosa *et al* 2005), BaTiO₃ (Patra *et al* 2003b), TiO₂ (Patra *et al* 2003b), and Gd₂O₃ (Guo *et al* 2004). The process of photon upconversion is a way to convert long-wavelength excitation radiation into shorter wavelength output radiation. Upconversion is one of the most studied nonlinear optical processes compared to second harmonic generation and two-photon absorption. The two most common excitation processes that lead to emission from the higher energy states to the terminating state are energy transfer upconversion (ETU) and excited state absorption (ESA). In both these cases, a simple cw diode laser can be used for the upconversion process, in contrast to expensive mode locked lasers used in two-photon upconversion in organic fluorophore. Therefore, efficient upconverting rare-earth doped nanocrystals can be good replacement of

organic dyes in two-photon confocal microscope imaging. The upconversion emission spectra and the pump-power dependence of luminescence intensities are essential to the understanding of excitation mechanism in rare-earth doped upconverting materials. It is often assumed that in such nonlinear processes the slope of the intensity versus pump power in double-logarithmic representation is equal to the number *n* of photons required to excite the emitting state. There is no report on the study of power dependence upconversion emission of BaTiO₃:Er³⁺ nanocrystals with changing dopant concentration. Therefore, there is plenty of scope for understanding the effect of dopant concentration and pump power on UPC luminescence efficiency of Er³⁺ doped BaTiO₃ nanocrystals.

2. Experimental

The synthesis procedure is described in our previous papers (Patra *et al* 2002, 2003b). Barium acetate (Ba(CH₃COO)₂·H₂O), titanium isopropoxide (Ti(OiPr)₄, from Fluka) and erbium acetate were used as the starting materials. First, Ba(Ac)₂ was dissolved in water and acetic acid under stirring condition. Then, the required amount of titania sol was slowly added to this solution under vigorous stirring at ambient temperature. A clear transparent sol was thus obtained. Then, the required amount of erbium acetate was added to this sol. To obtain emulsified sol droplets through water-in-oil (w/o) type emulsions, cyclohexane and sorbitan monooleate (Span 80, fluka) were used as the organic liquid (oil phase) and the non-ionic surfactant, respectively. The sol droplets formed in the process were then gelled by controlled addition of base. The gel particles were separated by centrifugation followed by washing with acetone and methanol. The product thus obtained

*Author for correspondence (msap@iacs.res.in)

was dried at 60°C in an air oven for 12 h. The dried materials were heated at different temperatures up to 1000°C. The particles were aggregated after heat treatment at high temperature. The crystallite sizes of the nanoparticles were calculated following the Scherrer's equation

$$D = K\lambda/\beta\cos\Theta,$$

where $K = 0.9$, D represents crystallite size (\AA), λ the wavelength of $\text{CuK}\alpha$ radiation and β the corrected half width of the diffraction peak. The crystalline phases of heat-treated powders were identified by X-ray diffraction (XRD). All peaks are matched well with the bulk BaTiO_3 , which could be indexed as the cubic structure of BaTiO_3 (JCPDS NO. 5-0626). We did not find any peak for tetragonal phase. We pressed the particles to form a smooth, opaque flat disk for optical study. The samples were irradiated with a diode laser tuned to 980 nm. A CCD-coupled spectrometer recorded the fluorescence spectra.

3. Results and discussion

Figure 1 shows the upconverted emission spectra of the 1 mol% Er^{3+} doped BaTiO_3 nanoparticles prepared at three different temperatures of heating, 700°C, 850°C and 1000°C. The upconversion luminance values are 343 Cd/m^2 , 1448 Cd/m^2 and 9487 Cd/m^2 for 700°C, 850°C and 1000°C heated samples, respectively. It is found that the upconversion emission intensity increases with increasing temperature of heating. The crystal phase (cubic) is same in all the samples and the estimated crystallite sizes are 30, 50 and 80 nm for 700, 850 and 1000°C, respectively. Therefore, the enhancement of the upconversion emission intensities related to the heating temperature is ascribed to two main factors: one is growth of the particles, which induces a decrease of the number of surface defects in the

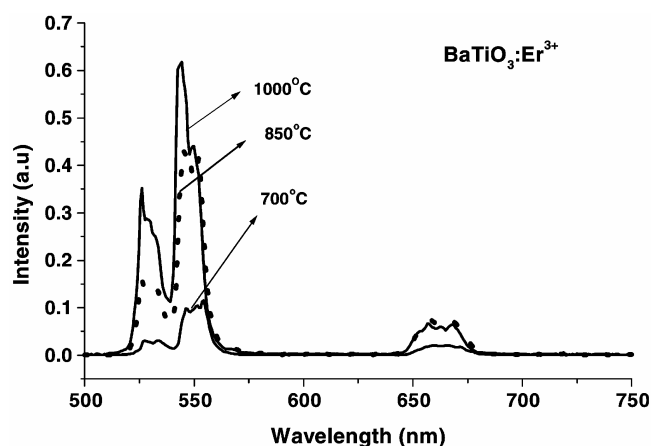


Figure 1. Upconverted emission spectra of 1 mol% Er^{3+} ions doped BaTiO_3 nanoparticles prepared at different temperatures, 700, 850 and 1000°C.

host; the second is the loss in the amount of organic residue and hydroxyl groups, which lowers the multiphonon relaxation rate. For the same concentration of dopant ions, the fraction of pairs will be different for different particles sizes. It is known that the probabilities for dopant pair-state formation depend on the particle size and the contributions of ions at the surface sites increases with decreasing size of particle. This could be another reason for increasing the upconversion luminance value with increasing the size for the same concentration because less dopant-pair formation occurs. Figure 2 shows the

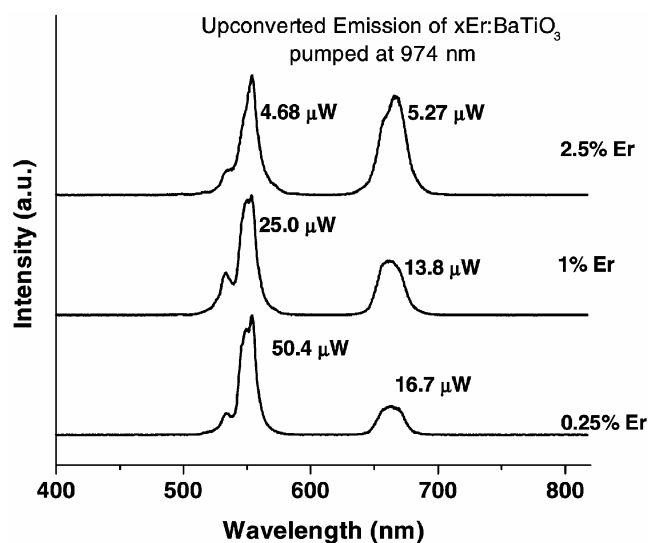


Figure 2. Upconverted emission spectra of different concentrations of Er^{3+} ions doped BaTiO_3 nanoparticles prepared at 1000°C.

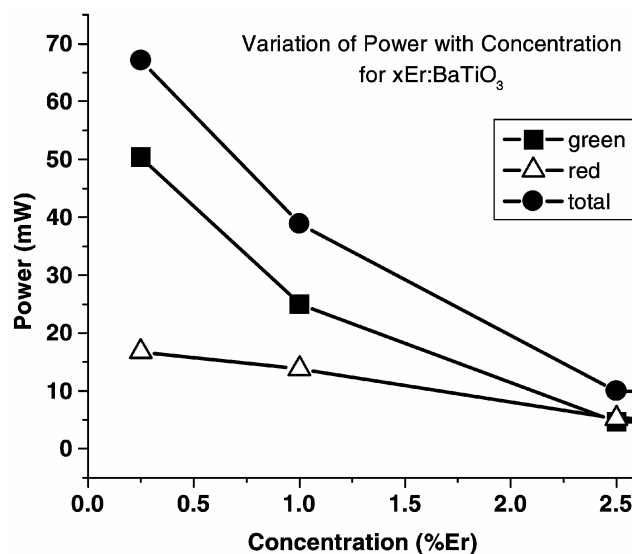


Figure 3. Variation of the luminescence value with changing concentration of Er^{3+} ions in BaTiO_3 nanocrystals prepared at 1000°C.

upconverted emission spectra of 1000°C heated different concentrations of Er³⁺ doped BaTiO₃ nanoparticles. The upconversion luminance values are 17130 Cd/m², 9487 Cd/m² and 1653 Cd/m² for 0.25, 1 and 2.5 mol% Er³⁺ doped BaTiO₃ nanocrystals, respectively. Here, we also observed that there is a significant drop in the overall intensity with increasing concentration of Er³⁺ ions. Figure 3 shows the variation of luminance value with changing concentration of Er³⁺ ions in BaTiO₃ nanocrystals. To our knowledge, no absolute luminance value of this system is reported. The absolute fluorescence intensity was measured with a Minolta LS-110 luminance meter, and the fluorescence was considered to be isotropic. The luminance is moderately high, considering the relatively moderate (850 mW) cw excitation power. Here, a significant drop in the overall intensity is observed with an increasing concentration of Er³⁺ ions due to concentration quenching non-radiative process. The intensity ratio of the green emission to that of the red emission decreases with increasing concentration of Er³⁺ ions. Since the size of the Er³⁺ ion (~0.10 nm) is almost intermediate between those of the Ba²⁺ ion (~0.14 nm) and Ti⁴⁺ ion (~0.06 nm), it seems equally likely that the Er³⁺ ions occupy the site of either ion in the BaTiO₃ lattice. At low concentration (0.25 mol%), the mean distance between the Er³⁺ ions is estimated by $R = 0.62/(N)^{1/3}$ to be 1.81 nm but for high concentration (2.5 mol%) the distance is 0.84 nm (Patra *et al* 2003b). Therefore, the erbium ions in low concentration Er³⁺-Er³⁺ distances are too far apart and at higher concentration, the distances between two Er³⁺ ions are shortening, thus leading to formation of Er³⁺ clusters (Quimby *et al* 1994). As a result, concentration-quenching processes will be the predominant non-radiative decay process at higher concentrations, as a result the emission intensity sharply decreased. Silver *et al* (2001) also showed that the upconversion process is most efficient for the larger particles. However, they suggested that resonance energy transfer is responsible for efficient upconversion in larger particles, because resonance energy transfers extend the lifetimes of the excited states of the rare-earth ions. The mechanism of the upconverted emission of Er³⁺ has been well established in the literature (Patra *et al* 2003b). To explain this phenomenon, we use the typical energy level diagram of Er³⁺ ions as shown in figure 4. The diode-laser wavelength (980 nm) matches the absorption transition between the ground state, ⁴I_{15/2}, and the excited level, ⁴I_{11/2}. After first-level excitation, the same laser pumps the excited atom from the ⁴I_{11/2} to the ⁴F_{7/2} level. Subsequent nonradiative relaxation populates the ⁴S_{3/2}/²H_{11/2} and the ⁴F_{9/2} levels. Bright green (550 nm) and red (670 nm) emission were observed due to the transitions ⁴S_{3/2} → ⁴I_{15/2} and ⁴F_{9/2} → ⁴I_{15/2}, respectively. At low dopant concentration, the ⁴S_{3/2}/²H_{11/2} levels decay radiatively to ⁴I_{15/2}. Therefore, the green emission has a higher intensity and this emission will mainly be contributed by the excited-state absorption (ESA) process. The luminescent lifetime of ⁴S_{3/2}/²H_{11/2} levels is shortened as a result of the cross-relaxation process between (²H_{11/2} → ⁴I_{9/2}) and (⁴I_{15/2} → ⁴I_{13/2}) transitions taking place at a higher concentration and the red emission is observed upon excitation at 980 nm. The study of emission intensity versus pump power is essential to understand the excitation mechanism in rare-earth doped upconverting materials. It is well known for an unsaturated mechanism, the intensity of the upconverted luminescence, I_{upc} , is proportional to some power, n , of the excitation intensity, I_i , i.e. $I_{\text{upc}} \propto I_i^n$, where $n = 2, 3, \dots$ is the number of pump photons required to populate the emitting state and is determined from the slope of the line of the graph of intensity versus pump power in a log-log plot. The pump power dependence of the emission bands at 550 and 670 nm were investigated on excitation intensity at 980 nm and the experimental data for 550 and 670 nm emission bands have been fit with a straight line with a slope of ~2, which confirms that these UPC emission lines are also a two-photon absorption process for low concentration of dopant. Figure 5a shows that the upconversion emission

Figure 4. The energy level diagram of Er³⁺ ion under infrared excitation.

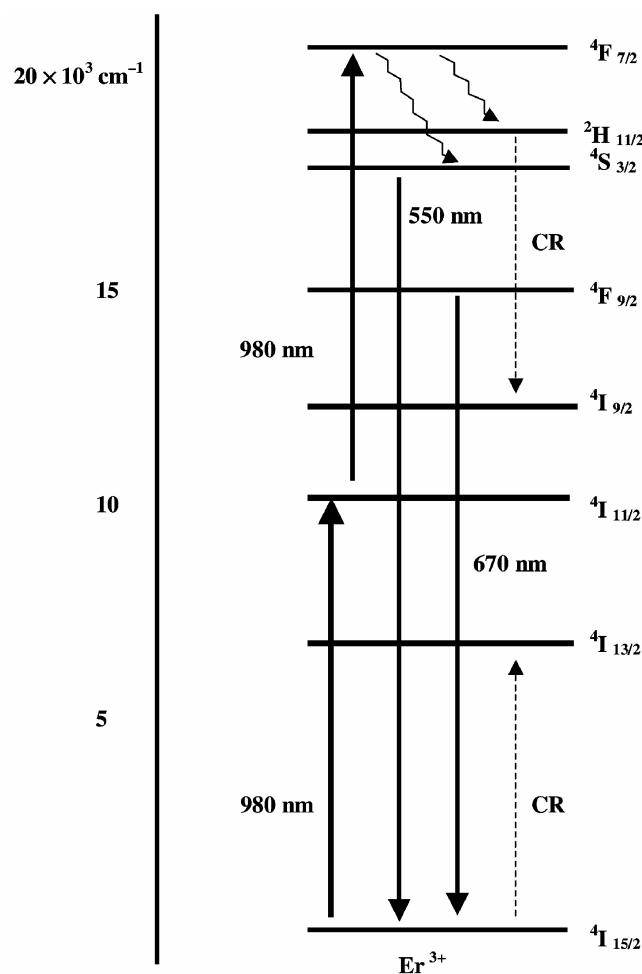


Figure 4. The energy level diagram of Er³⁺ ion under infrared excitation.

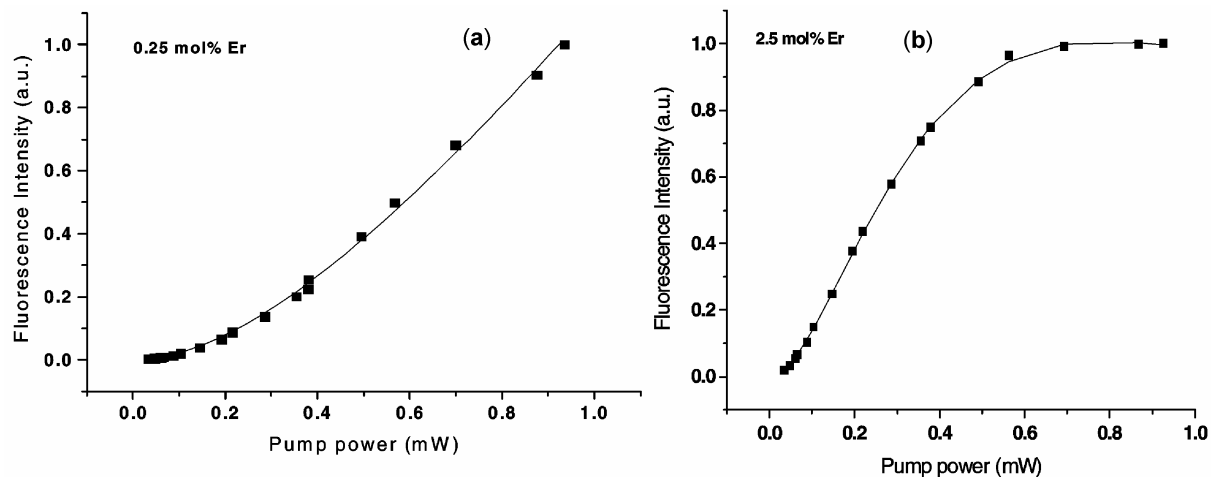


Figure 5. Power dependence upconverted emission intensity of 0.25 (a) and 2.5 (b) mol% Er^{3+} in BaTiO_3 nanoparticles heated at 1000°C .

intensity increases with increasing pump power in low concentration of dopant (0.25 mol%). It is worthwhile to mention that the unusual power-dependent upconversion luminescence (figure 5b) is observed at higher dopant concentration (2.5 mol%), which is a new and unprecedented result. We have seen that the upconversion emission intensity saturates at higher pump power (~ 0.7 W) for high concentration dopant (2.5 mol%). In case of parametric upconversion or higher order harmonic generations in quantum optics the cause of saturation may be due to depletion of pump power. In such processes the upconverted intensity exhibits n th order dependence on the pump power, which levels off to linear behaviour and conversion efficiency approaches unity. Unlike these systems the cause of saturation in ETU and ESA processes is the depletion of lower level populations. Therefore, in such cases at very high pump power the upconverted intensity should become constant or independent of pump intensity. In 1966, Singh and Geusic observed the ‘saturation’ phenomenon of upconversion of NdCl_3 single crystal for higher pump power. Recently, Pollnau *et al* (2000) also studied the physical nature of the saturation phenomenon in $\text{Cs}_3\text{Lu}_2\text{Cl}_9 : \text{Er}^{3+}$ and other crystals. There are several probabilities leading to the unusual power dependent upconversion luminescence behaviour. In order to analyse the UPC mechanism, we derived a relation between the fluorescence and the pump intensity by solving the rate equations based on the excitation and emission to understand the mechanism of the upconversion emission from $^4F_{9/2} \rightarrow ^4I_{15/2}$ level at 670 nm of 2.5 mol% Er^{3+} doped BaTiO_3 nanocrystals. We used a simple two-photon stepwise excited-state absorption process as shown in figure 6. In this case, depletion of the excited state is responsible for the relevant fluorescence upconversion. This is possible either by further excitation of the relevant level or nonradiatives de-excitation due to

change in temperature of the interaction volume. In both the cases, the depletion will be proportional to the pump power. In the former case, it is a direct dependence while in the latter case it is indirect dependence as the increase in temperature will be proportional to the absorbed energy in the interaction volume. The γ_{ij} is the decay rate or the transition probability from the i th to the j th level. $R_1 = \sigma_1 I_p / h \nu_p$ and $R_2 = \sigma_2 I_p / h \nu_p$ are the pump rates of the first and second steps, respectively. Here, σ_1 and σ_2 are the absorption cross sections of the first and second steps, respectively and ν_p the frequency of the pump light beam. In a simple manner the scheme can be depicted as a four-level system as shown in figure 6. If N_i is the population of the i th level and N the total ion density, the rate equations for describing this case are given as

$$N_1 R_1 - N_2 (R_1 + R_2 + \gamma_{21}) + N_3 (R_2 + \gamma_{32}) = 0, \quad (1)$$

$$R_2 N_2 - N_3 (R_2 + R_3 + \gamma_{31} + \gamma_{32}) = 0, \quad (2)$$

$$R_3 N_3 - N_4 \gamma_{41} = 0, \quad (3)$$

where R_3 is the rate of de-excitation of the third level to fourth level and is considered as proportional to pump power, I_p . The relation between the fluorescence intensity, I_f with I_p , in such a system will be given as

$$I_f = \frac{K I_p^2}{(A + B I_p + C I_p^2 + D I_p^3)}, \quad (4)$$

where the coefficients K , A , B and C are given as

$$\begin{aligned} K &= g N V \nu_f \sigma_1 \sigma_2 \gamma_{31} \gamma_{41} / h \nu_p^2, \\ A &= \gamma_{21} (\gamma_{31} + \gamma_{32}) \gamma_{41}, \\ B &= [(\sigma_2 + \sigma_3) \gamma_{21} + (2\sigma_1 + \sigma_2) \gamma_{31} + 2\sigma_1 \gamma_{32}] \gamma_{41} / h \nu_p, \\ C &= [(3\sigma_1 \sigma_2 + (2\sigma_1 + \sigma_2) \sigma_3)] / (h \nu_p)^2 \gamma_{41}, \\ D &= \sigma_1 \sigma_2 \sigma_3 / (h \nu_p)^3, \end{aligned}$$

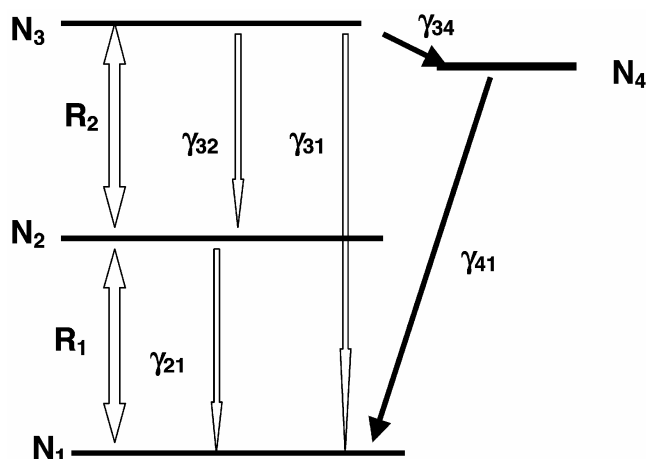


Figure 6. Four energy levels diagram depicting two-photon upconversion with excited state absorption (ESA) process with excited state depletion.

where σ_3 is the absorption cross-section from level three to level four, g the geometrical collection factor, N the rare-earth ion density in the sample, I_f the upconverted fluorescence intensity, I_p the pumping intensity and V the interaction volume. It is seen that (4) provides an excellent fit to the experimental data of 2.5 mol% Er-doped BaTiO₃ nanocrystals (figure 5b). However, in low concentration (0.25 mol%), the experimental data is fitted (figure 5a) with (4) where $C = 0$ and $D = 0$. Our analysis clearly reveals that upconversion emission and pump power dependence emission are sensitive to dopant concentration. It is demonstrated that derived expression fits excellently to the experimental data. We have again confirmed that upconversion process in all these samples are due to two-photon excited-state absorption (ESA) process.

4. Conclusions

Here, we demonstrated the role of dopant concentration and pump power on upconversion emission efficiency of Er³⁺

doped BaTiO₃ nanocrystals. We have shown that the overall upconversion luminescence intensity decreases with an increasing concentration of the Er³⁺ ions and the concentration quenching is responsible for the decrease in overall intensity. We have also confirmed that the upconversion process follows two-photon ESA process.

Acknowledgements

The Department of Science and Technology (NSTI), is acknowledged for financial support. (SS) and (TS) thank CSIR for fellowships.

References

- Dowing E, Hesselink L, Ralston J and Macfarlane R 1996 *Science* **273** 1185
- Guo H, Dong N, Yin M, Zhang W, Lou L and Xia S 2004 *J. Phys. Chem.* **B108** 19205
- La Rosa-Cruz E De, Diaz-Torres L A, Rodriguez-Rojas R A, Meneses-Nava M A, Barbosa-Garcia O and Salas P 2003 *Appl. Phys. Lett.* **83** 4903
- La Rosa E De, Salas P, Desirena H, Angeles C and Rodriguez R A 2005 *Appl. Phys. Lett.* **87** 241912
- Matsuura D 2002 *Appl. Phys. Lett.* **81** 4526
- Pandozzi F, Vetrone F, Boyer J C, Naccache R, Capobianco J A, Speghini A and Bettinelli M 2005 *J. Phys. Chem.* **B109** 17400
- Patra A, Friend C S, Kapoor R and Prasad P N 2002 *J. Phys. Chem.* **B106** 1909
- Patra A, Friend C S, Kapoor R and Prasad P N 2003a *Appl. Phys. Lett.* **83** 284
- Patra A, Friend C S, Kapoor R and Prasad P N 2003b *Chem. Mater.* **15** 3650
- Pollnau M, Gamelin D R, Luthi S R, Gudel H U and Hehlen M P 2000 *Phys. Rev.* **B61** 3337
- Quimby R S, Miniscalco W J and Thompson B 1994 *J. Appl. Phys.* **76** 4472
- Silver J, Martinez-Rubio M I, Ireland T G, Fern G R and Withnall R 2001 *J. Phys. Chem.* **B105** 948
- Silversmith A J, Lenth W and Macfarlane R M 1987 *Appl. Phys. Lett.* **51** 1977
- Singh S and Geusic J E 1966 *Phys. Rev. Lett.* **17** 865